Intrinsic rate of electron transfer in the diffusional quenching of trans-stilbene S1 by fumaronitrile

ARTICLE *in* THE JOURNAL OF PHYSICAL CHEMISTRY · JANUARY 1989

Impact Factor: 2.78 · DOI: 10.1021/j100339a041

2 AUTHORS, INCLUDING:

Stephen A. Angel
Washburn University
7 PUBLICATIONS **86** CITATIONS

$$f_{ox} = \left(\frac{h + 0.5}{h - 0.5}\right)\frac{2q}{c}$$

For $h = 1.5$, $q = 0.0002$, and $c = 0.024$, we find that $f_{ox} = 3\%$. For Ce waves under these conditions ($[Ce]_{total} = 3$ mM), the observed steady state has $f_{ox} = 10\%$, in reasonable agreement with the theoretical value.

To describe wave propagation in thin layers of BZ reagent, we must introduce diffusion terms into system (A9)-(A10), which becomes

$$\frac{\partial x}{\partial t} = \epsilon\frac{\partial^2 x}{\partial s^2} + \frac{1}{\epsilon}\left[x(1 - x) - hz\frac{x - q}{x + q} - \kappa_{-5}u^2\right] \quad \text{(A11)}$$

$$\frac{\partial z}{\partial t} = \delta\epsilon\frac{\partial^2 z}{\partial s^2} + [2(x - \kappa_{-5}u^2) - z] \quad \text{(A12)}$$

where $\delta = D_z/D_x$, the ratio of diffusion constants for catalyst and $HBrO_2$. In (A11)-(A12) the dimensionless spatial variable s is defined by

$$s = \frac{k_1 B}{(k_5 HAD_x)^{1/2}}(\text{space})$$

In the text we present numerical solutions of system (A11)-(A12) for the special case $\delta = 1$.

Registry No. Ce, 7440-45-1; BrO_3^-, 15541-45-4; malonic acid, 141-82-2.

Intrinsic Rate of Electron Transfer in the Diffusional Quenching of *trans*-Stilbene S_1 by Fumaronitrile

Stephen A. Angel and Kevin S. Peters*

Department of Chemistry and Biochemistry, University of Colorado, Boulder, Colorado 80309-0215
(Received: April 12, 1988; In Final Form: June 16, 1988)

The quenching of the first excited singlet state of *trans*-stilbene (S_1) by fumaronitrile in acetonitrile has been examined by picosecond laser spectroscopy. From the time dependence of the rate constant for the quenching of S_1, the intrinsic rate of the electron transfer can be separated from the diffusional contribution. The rate of electron transfer is $k_{et} = 1.9 \times 10^{12}$ M^{-1} s^{-1}. From the time dependence of the formation of the resulting ion pair, it is concluded that the electron transfer occurs when the molecules are in contact.

Introduction

The photochemistry of *trans*-stilbene has been the focus of numerous investigations in recent years. The dynamics of the excited-state isomerization have been of particular interest, as this system has been used as a test of various theoretical models for the coupling of the solvent friction to the large-amplitude motion of the isomerization.[1-4] *trans*-Stilbene also displays a very rich photochemistry. As early as 1902, the photodimerization of stilbene to give tetraphenylcyclobutane was reported.[5] In 1968, Chapman observed[6] an inverse temperature dependence upon the quantum yield for the photocycloaddition of *trans*-stilbene with tetramethylethylene. Weak exciplex emission was observed in the photocycloaddition of *trans*-stilbene with 2,5-dimethyl-2,4-hexadiene.[7] To account for these observations, the intervention of an exciplex was proposed.[6,7] The role of the exciplex in stilbene's photochemistry has been thoroughly addressed by Lewis and co-workers.[7] From these and numerous other studies, it is found that photocycloaddition reactions of stilbene occur within the exciplex.

Recently we reported a series of investigations into the photochemistry of *trans*-stilbene in the presence of fumaronitrile.[8-10] This system displays strong exciplex emission in nonpolar solvents but does not undergo a photocycloaddition reaction. The 355-nm irradiation of the charge-transfer band formed between stilbene and fumaronitrile directly produces a contact ion pair in all solvents examined, ranging from nonpolar solvents such as benzene to polar solvents such as acetonitrile. In nonpolar solvents the contact ion pair decays to the ground-state reactants by either back electron transfer or emission. In aprotic polar solvents there is a competition in the decay of the contact ion pair between either back electron transfer or ion-pair separation to produce solvent-separated ion pairs. The rates for these competing decay processes have been examined as a function of solvent, added salts, and temperature.[8-10]

Since contact ion pairs are directly produced upon irradiation of the stilbene/fumaronitrile charge-transfer band, a question arises as to the nature of the ion pair formed in the diffusional quenching of the first excited singlet state of stilbene by fumaronitrile. This reaction is estimated to be 18 kcal/mol exothermic in acetonitrile.[7] Thus it is conceivable that the quenching may involve long-range electron transfer to form solvent-separated ion pairs which can have a very different chemistry from that of the contact ion pair. In this paper we examine the picosecond dynamics of the diffusional quenching of the excited singlet state of *trans*-stilbene by fumaronitrile. We analyze the results within the context of the Marcus formalism for electron-transfer processes that are coupled to translational diffusion and obtain the intrinsic rate for electron transfer.[11] Finally, the nature of the ion pair that is produced upon electron transfer is addressed.

Experimental Section

This section is subdivided by three experiments: the apparatus for picosecond absorption kinetics is reviewed, the electrochemical method and equations used to determine diffusion coefficients for *trans*-stilbene and fumaronitrile are presented, and a technique for estimating the initial concentration of the *trans*-stilbene/fu-

(1) Zeglinski, D. M.; Waldeck, D. H. *J. Phys. Chem.* **1988**, *92*, 692.
(2) Rothenberger, G.; Negus, D, K.; Hochstrasser, R. M. *J. Chem. Phys.* **1983**, *79*, 5360.
(3) Courtney, S. H.; Fleming, G. R. *J. Chem. Phys.* **1985**, *83*, 215.
(4) Sundstrom, V.; Gillbro, T. *Chem. Phys. Lett.* **1984**, *109*, 538.
(5) Ciamician, G.; Silber, P. *Chem. Ber.* **1902**, *35*, 4128.
(6) Chapman, O. L.; Adams, W. R. *J. Am. Chem. Soc.* **1968**, *90*, 2333.
(7) Lewis, F. D. *Acc. Chem. Res.* **1979**, *12*, 152.
(8) Goodman, J. L.; Peters, K. S. *J. Am. Chem. Soc.* **1985**, *107*, 6459.
(9) Goodman, J. L.; Peters, K. S. *J. Am. Chem. Soc.* **1985**, *107*, 1441.
(10) Goodman, J. L.; Peters, K. S. *J. Phys. Chem.* **1986**, *90*, 5506.
(11) Marcus, R. A.; Siders, P. *J. Phys. Chem.* **1982**, *86*, 622.

0022-3654/89/2093-0713$01.50/0

maronitrile ground-state charge-transfer complex is described. Finally, there is a summary of the chemical solutions employed.

Picosecond Absorption Spectrometer. An 18-nJ, 600-nm, 1-ps pulse is produced by a rhodamine 6G dye laser, pumped by a frequency-doubled, moded-locked, Nd:YAG laser (Spectra-Physics 3000). The theory and design of the pulsed dye amplifier have been previously presented.[12] In this experiment, a Q-switched Nd:YAG laser (Quanta Ray DCR-2) is synchronously triggered by the mode-locked laser to establish temporal overlap of the dye laser pulse with the amplifier. The 150-mJ, 532-nm, 10-ns output pulse is split into 10/10/80%, respectively, to longitudinally excite R640/methanol flowing in three successive cells. Crystal violet/ethylene glycol jets absorb spontaneous emission between the first two dye cells. The output of the amplifier is a 2.0-mJ, 600-nm pulse with a temporal width ranging from 1 to 2 ps.

The 600-nm pulse is frequency-doubled to 300 nm using a 5-mm KDP crystal with 5% efficiency. The remainder of the 600-nm pulse is focused into a 5-cm cell of H_2O/D_2O resulting in a continuum of usable white light between 450 and 750 nm. A narrow band-pass filter coupled with a polarizer at the magic angle determines the wavelength and polarization of the probe pulse. This probe pulse is delayed with respect to the 300-nm pump pulse using a stepping motor driven delay line.

The probe pulse is split into two beams, an I and I_0 pulse, which are detected by two photodiodes in tandem with boxcar integrators (SRI). The data from the boxcar integrators is transferred to a laboratory computer (PDP 11/23). At each time delay, the difference of the log (I_0/I) with excitation and log (I_0/I) without excitation is averaged over 200 laser pulses. The sample is continuously flowed to prevent the buildup of photoproducts.

Measurement of Diffusion Coefficients. Diffusion coefficients for *trans*-stilbene (TS) and fumaronitrile (FN) in acetonitrile were determined by using the chronocoulometric mode on a BAS 100 electrochemical analyzer. This mode yields the slope of the charge with respect to the square root of time according to the integrated Cottrell equation.[13]

$$Q = 2nFAD_B^{1/2}C_Bt^{1/2}/\pi^{1/2} \quad (1)$$

In eq 1, n is the number of electrons transferred, F is Faraday's constant, A is the effective area of the electrode, C_B is the concentration of solute B, and D_B is the diffusion coefficient of solute B.

The diffusion of ferrocene (FC) in acetonitrile is used as a standard.[14] The diffusion coefficients of TS or FN are then obtained with reference to ferrocene through eq 2.

$$D_{TS} = [\{\text{slope TS}/\text{slope FC}\}\{D_{FC}\}^{1/2}\{C_{FC}/C_{TS}\}]^2 \quad (2)$$

The concentrations employed were $C_{FC} = 2.15$ mM, $C_{TS} = 2.01$ mM, and $C_{FN} = 1.98$ mM. The diffusion coefficient of ferrocene is $D_{FC} = 2.4 \times 10^{-5}$ cm^2/s.

trans-Stilbene/Fumaronitrile Charge-Transfer Complex. A Perkin-Elmer, Lambda 3, UV/vis spectrometer at 340 nm was used to determine the Hildebrand/Benesi equilibrium constant[15] for the ground-state charge-transfer complex between TS and FN in acetonitrile. Various concentrations of TS and FN were used in an approximate ratio of 80/1. The initial concentration of FN was assumed not to change due to complex formation. Absorption due to TS at 340 nm was determined with successive approximations of the Hildebrand/Benesi equation and subtracted from the observed absorption at this wavelength. The absorption at 300 nm was found to decrease slightly as the FN concentration increased; this is attributed to the charge-transfer complex having a somewhat smaller extinction coefficient than TS. The equilibrium constant for the formation of the charge-transfer complex is $K_{eq} = 0.13 \pm 0.06$ M^{-1}.

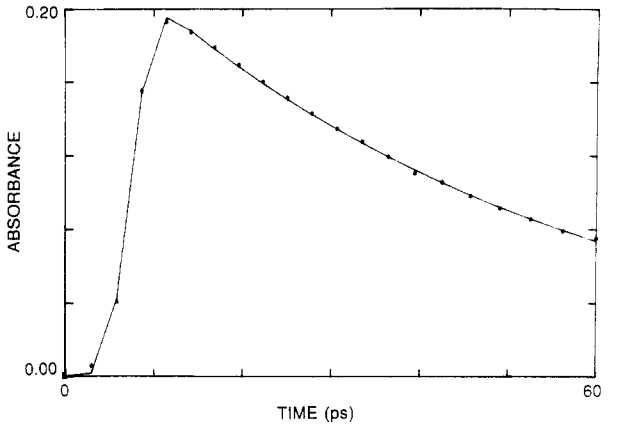

Figure 1. Decay dynamics of S_1 for *trans*-stilbene (30 μM) in acetonitrile following 300-nm excitation and monitoring at 570 nm. Points are experimental data. Curve is calculated from eq 3 using $\tau = 48.8$ ps, $\sigma = 1.9$ ps, $c = 7.0$ ps, and ABS(0) = 0.22.

Solutions. *trans*-Stilbene was obtained from Aldrich and recrystallized from ethanol. The fumaronitrile was obtained from Aldrich and sublimed. The acetonitrile used was Fisher HPLC grade. In the absence of TS, neither acetonitrile nor FN in acetonitrile absorbs at 300 nm.

The concentrations of FN were determined by mass/volume and varied from 0.05 to 0.9 M unless otherwise noted. The concentration of TS was determined by its optical density at 300 nm and was normally 30 μM. The experimentally measured 300-nm extinction coefficient of TS in acetonitrile is 2.66×10^4 M^{-1} cm^{-1}.

Results and Discussion

The dynamics of the first excited singlet state (S_1) of *trans*-stilbene (TS) in acetonitrile produced upon 300-nm excitation are monitored at 570 nm, near the absorption maximum of the $S_n \leftarrow S_1$ transition,[16] Figure 1. The kinetics of the decay of S_1 may be fit to a single exponential. Convolution of a single-exponential decay with a Gaussian instrument response function results in an equation with four determinable parameters:[17]

$$\text{ABS}(t) = [\text{ABS}(0)(2\pi\sigma^2)^{-1/2}] \exp[-t/\tau] \times \int_0^t \exp[-(x-c)^2/(2\sigma^2)] \exp[x/\tau]\, dx \quad (3)$$

In this equation, τ is the lifetime of S_1, σ_2 represents the time variance of the Gaussian instrument response function,[18] c is the time for the overlap of the excitation pulse and the probe pulse to reach its maximum, and ABS(0) is the absorption at $t = 0$ if the excitation and probe pulses were infinitely fast.

Figure 1 depicts an average of four pump/probe experiments of TS in acetonitrile subject to a least-squares fit of eq 3 to the experimental data. The parameters giving the best fit are $\tau = 48 \pm 3$ ps, $\sigma = 1.9 \pm 0.4$ ps, $c = 7.0 \pm 0.4$ ps, and ABS(0) = 0.22 ± 0.02. For each experimental point in time there is a calculated absorption point; these points are sequentially connected to one another with a line. The same S_1 decay kinetics are observed at 590 and 610 nm.

In the absence of a quencher, S_1 of TS decays by isomerization upon the excited-state energy surface followed by internal conversion to the ground-state surface. However, in the presence of fumaronitrile (FN), an electron may be transferred from S_1 to FN to produce the radical cation of *trans*-stilbene (TS^+) and the radical anion of fumaronitrile (FN^-).[8] The reaction is estimated to be 18 kcal/mol exothermic in acetonitrile. It is thus anticipated that increasing the concentration of FN will lead to a decrease in lifetime of S_1. The decay kinetics of S_1 in the presence of

(12) Koch, T. L.; Chiu, L. C.; Yariv, A. *Opt. Commun.* **1982**, *40*, 364.
(13) Bard, A. J.; Faulkner, L. *Electrochemical Methods*; Wiley: New York, 1980.
(14) Kuwaha, T.; Bublitz, D. E.; Hoh, G. *J. Am. Chem. Soc.* **1960**, *82*, 5811.
(15) Benesi, H. A.; Hildebrand, J. H. *J. Am. Chem. Soc.* **1949**, *71*, 2703.
(16) Hochstrasser, R. M. *Pure Appl. Chem.* **1980**, *52*, 2683.
(17) Demas, J. N. *Excited State Lifetime Measurements*; Academic: New York, 1983.
(18) McQuarrie, D. A. *Statistical Mechanics*; Harper & Row: New York, 1976.

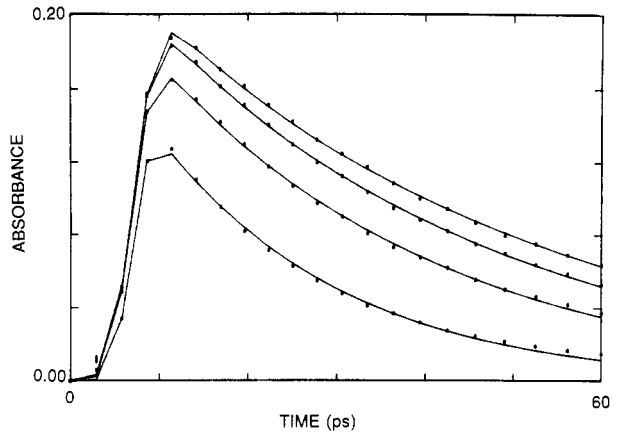

Figure 2. Dynamics of the quenching of S_1 as a function of fumaronitrile (FN) concentration, in acetonitrile, following 300-nm excitation and monitoring at 570 nm. Points are experimental data. Concentrations of FN are (top to bottom) 0.049 (A), 0.101 (B), 0.191 (C), and 0.463 M (D). *trans*-Stilbene concentration is 30 μM. Curves A–D are calculated from eq 3 using the following parameters: (A) τ = 43 ps, σ = 2.1 ps, c = 7.1 ps, ABS(0) = 0.214. (B) τ = 38 ps, σ = 1.9 ps, c = 7.1 ps, ABS(0) = 0.208. (C) τ = 31 ps, σ = 2.0 ps, c = 6.9 ps, ABS(0) = 0.193. (D) τ = 20 ps, σ = 1.6 ps, c = 7.0 ps, ABS(0) = 0.155.

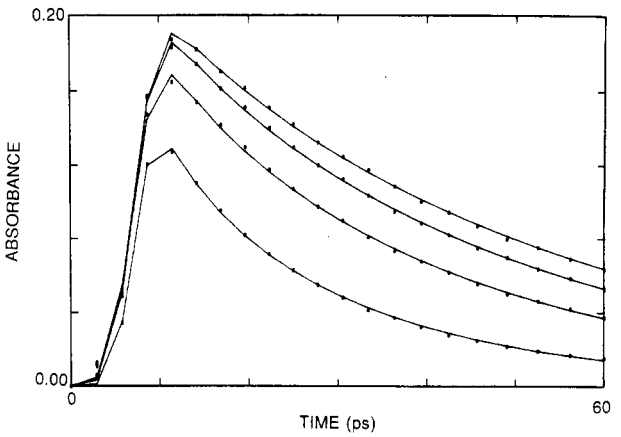

Figure 3. Dynamics of the quenching of S_1 as a function of fumaronitrile (FN) concentration, in acetonitrile, following 300-nm excitation and monitoring at 570 nm. Points are experimental data. Concentrations of FN are (top to bottom) 0.049 (A), 0.101 (B), 0.191 (C), and 0.463 M (D). *trans*-Stilbene concentration is 30 μM. Curves A–D are calculated from eq 5 using the following parameters: (A) ABS(0) = 0.22, R = 8.3 Å, σ = 2.1 ps, c = 7.2 ps. (B) ABS(0) = 0.22, R = 8.6 Å, σ = 2.0 ps, c = 7.2 ps. (C) ABS(0) = 0.22, R = 8.7 Å, σ = 2.1 ps, c = 7.1 ps. (D) ABS(0) = 0.20, R = 8.4 Å, σ = 1.8 ps, c = 7.3 ps.

varying concentrations of FN (0.049–0.463 M) in acetonitrile are shown in Figure 2. Each experimental decay curve is an average of three pump/probe experiments. These kinetic data are then subject to a least-squares fit to eq 3; these fits are pseudo first order with respect to FN at concentrations varying from 0.049 to 0.463 M in a solution of 30 μM TS in acetonitrile. The second-order rate constant for the quenching of S_1 by FN, determined from the ratio of the pseudo-first-order rate constants to FN concentration, is $(6.20 \pm 0.04) \times 10^{10}$ M^{-1} s^{-1}.

Equation 3, which assumes a time-independent rate constant, reproduces well the decay kinetics of S_1 in the absence of FN. However, for the FN quenching experiments the quality of the fit decreases with increasing FN concentration. This is most obvious in the 0.48 M FN data where the calculated curve overestimates the absorbances at early times and underestimates the absorbances at later times. Employing a linear least-squares analysis of the log of the absorbance versus time, as the time interval narrows from 23–60 ps to 37–60 ps, the second-order rate constant increases by 17%. Therefore, the rate constant for the quenching of S_1 by FN is time-dependent.

The origin of the time-dependent rate constant for the quenching of S_1 by FN is the result of the initial conditions of the experiment.[19] Prior to the excitation of TS, there is an equilibrium distribution of quenchers about TS. Following excitation, there is an immediate depletion of quenchers in the vicinity of S_1 due to electron transfer, which reduces the local concentration of FN and causes a decrease in the subsequent observed rate of quenching. This decreasing concentration of FN about S_1 generates a concentration gradient, thereby causing a net diffusion of FN toward S_1 which may eventually lead to a steady-state concentration profile. A mathematical description for this process has been developed. A time-dependent bimolecular rate constant is predicted for diffusion-controlled reactions according to the equation[20,21]

$$k(t) = 4\pi RDN_A[1 + R(\pi Dt)^{-1/2}] \quad (4)$$

where N_A is Avogadro's number, D is the sum of the solute diffusion coefficients in the solution, and R is the radius of reaction such that the concentration of the reactants separated by $r \leq R$ is zero.[20]

The diffusion coefficients for TS and FN in acetonitrile were determined by electrochemical methods. The diffusion coefficients for TS and FN are 2.4×10^{-5} and 6.8×10^{-6} cm^2/s, respectively. Thus, D is 3.1×10^{-5} cm^2/s.

The decay of S_1 in the presence of FN was modeled as two competing reactions involving a time-independent process k_1, corresponding to the S_1 decay in the absence of FN, and a time-dependent process $k(t)$ due to diffusional quenching. Convolution of the two competing decay kinetics with a Gaussian instrument response function leads to

$$\mathrm{ABS}(t) = [\mathrm{ABS}(0)/(\sigma(2\pi)^{-1/2})] \exp\{-t(k_1 + a)\} \times \int_0^t \exp\{-(x - c)^2/(2\sigma^2)\} \exp\{x(k_1 + a)\} \exp\{-2b(t - x)^{1/2}\}\, dx \quad (5)$$

where $a = 4\pi RDN_A[\mathrm{FN}]_0$, $b = 4(\pi D)^{1/2}R^2N_A[\mathrm{FN}]_0$, k_1 = (49 ps)$^{-1}$, $[\mathrm{FN}]_0$ is the initial molar concentration of FN, and R is a variable.

The least-squares fit of eq 5 to the data is shown in Figure 3. The value of R is found to range from 8.3 to 8.7 Å. The calculated center-to-center distance for TS to FN along the diagonal axis of each molecule is approximately 8.7 Å in the absence of the terminal atoms' van der Waals radii.

Although this analysis is able to reproduce the experimental data, the assumptions employed in its development may not be valid for the present system. The first assumption is that the intrinsic rate of the reaction is infinitely fast, causing the observed dynamics to result only from translational diffusion. On the 1–5-ps time scale, however, diffusional motion may not make a major contribution to the observed kinetics. Rather, initially, the kinetics may be governed by the intrinsic rate of the electron transfer. The second assumption is that the concentration of reactants is zero for $r \leq R$, which again may not be valid. Relaxing the conditions that the concentration of the reactants inside a sphere of radius R is zero and that the rate of electron transfer is infinitely fast produces a more general time-dependent rate constant:[11,20,22]

$$k(t) = [1/(k_{et}^{-1} + k_d^{-1})][1 + (k_{et}/k_d) \exp(y^2) \operatorname{erfc}(y)] \quad (6)$$

where erfc (y) is the complementary error function

$$\operatorname{erfc}(y) = (2\pi^{-1/2}) \int_y^\infty \exp(-u^2)\, du$$

$y = (Dt)^{1/2}R^{-1}(1 + (k_{et}/k_d))$, and D and R have been previously defined. This formalism has recently been developed and discussed by Marcus in his analysis of highly exothermic electron-transfer

(19) Butler, P. R.; Pilling, M. J.; Rice, S. A.; Stone, T. J. *Can. J. Chem.* **1977**, *55*, 2124.
(20) Collins, F. C.; Kimball, G. *J. Colloid Sci.* **1949**, *4*, 425.
(21) Smoluchowski, M. *Z. Phy. Chem.* **1917**, *92*, 129.
(22) Noyes, R. M. *Prog. React. Kinet.* **1961**, *1*, 129.

TABLE I: Calculated Time Dependence of the Rate, from Eq 7, for the Quenching of *trans*-Stilbene S_1 by Fumaronitrile, with $k_{et} = 1.929 \times 10^{12}$ M^{-1} s^{-1} and $k_d = 2.0 \times 10^{10}$ M^{-1} s^{-1}

time, ps	rate, $\times 10^{12}$ M^{-1} s^{-1}	time, ps	rate, $\times 10^{12}$ M^{-1} s^{-1}
0.0	1.929	11.4	0.069
2.9	0.117	14.1	0.064
5.8	0.088	16.9	0.059
8.7	0.076	19.6	0.057

reactions.[11] When the reaction is initiated at $t = 0$, the system is at equilibrium and the rate of electron transfer is $k(0) = k_{et}$. As the reaction proceeds, the effect of the intrinsic rate of electron transfer is progressively masked by diffusion until steady-state conditions are achieved. This is given by $k(\infty) = (k_{et}^{-1} + k_d^{-1})^{-1}$, where k_d is the diffusion rate constant; $k_d = 4\pi RDN_A$.

Employing this formalism, the experimental data for FN quenching was analyzed by a least-squares fit where $k(t)$ is defined by eq 6:

$$\mathrm{ABS}(t) = [\mathrm{ABS}(0)(2\pi\sigma^2)^{-1/2}][\exp\{-(k_1 + a)\}] \times \left[\int_0^t dx\, \exp\{-(x - c)^2/2\sigma^2\} \exp\left\{(k_1 + a)x - b\int_0^{t-x} d(t - x)'\, \exp(y^2)\, \mathrm{erfc}\,(y)\right\}\right] \quad (7)$$

and $a = [\mathrm{FN}](k_{et}^{-1} + k_d^{-1})^{-1}$, $b = k_{et}[\mathrm{FN}](k_d/k_{et} + 1)^{-1}$, and $y = (Dt)^{1/2}R^{-1}(1 + k_{et}/k_d)$. The variables to the fit were k_{et} and ABS(0); the remaining parameters were set constant at $\sigma = 2.0$ ps, $c = 7.2$ ps, and R ranged from 8 to 12 Å in increments of 0.5 Å. The best fit occurs when $k_{et} = 1.9 \times 10^{12}$ M^{-1} s^{-1} and $R = 8.5$ Å. As expected[22] from a first-term asymptotic expansion of $\exp(y^2)$ erfc (y), which is valid for $k_{et} \gg k_d$, the quality of the fit is virtually identical with that found when k(t) is expressed by eq 4.

Given the above parameters, $k(t)$ was calculated as a function of t, Table I. From 0 to 2.9 ps, $k(t)$ is found to decrease by a factor of 17 from 1.9×10^{12} M^{-1} s^{-1} to 0.11×10^{12} M^{-1} s^{-1}. Although a finite instrument response unfortunately prohibits a direct experimental measurement of $k(t)$ during the first few picoseconds, there is another observation which supports this fast rate of electron transfer. In Figure 3 it is observed that there is a decrease in the maximum absorbance of S_1 with increasing FN concentration. To estimate a normalized maximum absorption decrease, (1 − ABS), due to a large k_{et}, eq 8 was employed with

$$\mathrm{ABS}(t=8\ \mathrm{ps}) = \exp\left\{-\int_0^8 k(t)\, dt\right\} \quad (8)$$

$k(t)$ given by eq 6. Assuming $k_{et} = 1.9 \times 10^{12}$ M^{-1} s^{-1} in eq 7, for 1 M FN, the calculated decrease in S_1 absorbance at 8 ps is 67%. The value of 8 ps represents the maximum absorbance at 1 M FN. The experimentally observed absorbance decrease at 8 ps is 65 ± 10% per mole of FN.

A question raised in the Introduction is whether the quenching process involves long-range electron transfer to produce solvent-separated ion pairs or short-range electron transfer to produce contact ion pairs. From the analysis of the diffusional quenching data, it was deduced that the distance of the electron transfer is 8.5 Å. However, the model used to develop eq 4 and 6 assumed isotropic electron transfer which probably does not accurately represent the present experimental system. More direct information regarding the nature of the electron transfer can be obtained from the resulting ion-pair dynamics which can be observed at 480 nm, the absorption maximum of TS^+. From our previous studies we have observed that TS^+/FN^- ion pairs have different kinetic behavior.[9] The contact ion pair is found to undergo back electron transfer to form ground-state reactants in competition with ion-pair separation to form solvent-separated ion pairs on the 150-ps time scale. In contrast, the solvent separated ion pair is found to be stable on the 20-ns time scale. Thus, in order to a ascertain whether electron transfer occurs over short or long range, we will assume that there are two limiting regimes for electron transfer: one where only contact ion pairs (CIP) are formed and one where only solvent-separated ion pairs (SSIP) are formed. These two limits lead to Schemes I and II. In Scheme I, the CIP is formed through irradiation of the charge-transfer band and through short-range electron transfer; formation of the SSIP is in competition with CIP's decay back to the ground state, GS. In Scheme II, the SSIP is produced through both long-range electron transfer, k_2, and through separation of the CIP, k_3, which was initially produced through irradiation of the charge-transfer band.

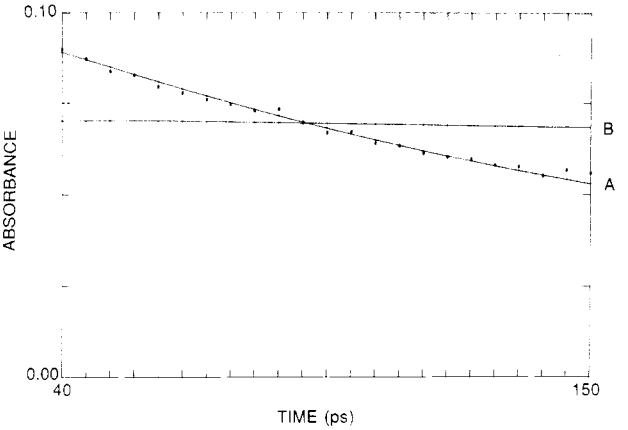

Figure 4. Dynamics of *trans*-stilbene radical cation, monitored at 480 nm, following 300-nm excitation of a 30 μM *trans*-stilbene/0.886 M FN in acetonitrile. Points are experimental data. Curve A is the calculated kinetics for Scheme I. Curve B is the calculated kinetics for Scheme II.

SCHEME I

$$S_1 \rightarrow GS \qquad k_1$$
$$S_1 + FN \rightarrow CIP \qquad k_2$$
$$CIP \rightarrow SSIP \qquad k_3$$
$$CIP \rightarrow GS \qquad k_4$$

SCHEME II

$$S_1 \rightarrow GS \qquad k_1$$
$$S_1 + FN \rightarrow SSIP \qquad k_2$$
$$CIP \rightarrow SSIP \qquad k_3$$
$$CIP \rightarrow GS \qquad k_4$$

Given the two models presented in Schemes I and II, it is possible to calculate the time-dependent absorption changes of TS^+ at 480 nm since all the kinetics parameters in the two schemes are known. At $t = 0$ the concentration of CIP produced upon irradiation of the charge-transfer band can be estimated from the equilibrium constant for the formation of the charge-transfer complex, obtained from the Hildebrand/Benesi experiment. It is noted that the 480-nm absorption reflects a combination of CIP and SSIP dynamics as TS^+ absorption is insensitive to the counteranion. The kinetic constants employed in the calculation of the time-dependent absorption changes of TS^+ are $k_1 = (49\ \mathrm{ps})^{-1}$, k_2 is $k(t)$ from eq 4 with $R = 8.5$ Å, $k_3 = (800\ \mathrm{ps})^{-1}$, and $k_4 = (170\ \mathrm{ps})^{-1}$.[23] The SSIP does not decay on the time scale of the experiment (20 ns).

Figure 4 shows the data from an experiment which monitors 480-nm absorbance from 40 to 150 ps. The FN concentration was 0.886 M. Both Schemes I and II are fit to the experimental data by using the aforementioned constants; only ABS(0) was allowed to vary. Clearly, Scheme I gives a superior fit to the experimental data, thereby suggesting that electron transfer from S_1 to FN occurs when the two molecules are in contact. Furthermore, given the 8.5-Å electron-transfer distance, it would

(23) O'Driscoll, E.; Peters, K. S., submitted for publication in *J. Phys. Chem.*

appear that the electron transfer occurs when the two molecules are edge to edge[24] and not in the π-complex form which would involve a distance of approximately 3.5 Å.[25]

Conclusions

From the time dependence of the observed rate constant for the quenching of the first excited singlet state of *trans*-stilbene by fumaronitrile in acetonitrile, it is possible to separate the intrinsic rate of electron transfer from the rate of diffusion. With the time resolution afforded by the picosecond absorption spectrometer, diffusional processes are no longer rate limiting. Thus, for a reaction that involves intermolecular electron transfer, it is now possible to examine the intrinsic rate of electron transfer as a function of energy change. We are currently examining the rate of electron transfer from the S_1 of *trans*-stilbene to a variety of electron-poor olefins in order to examine the Marcus theory for electron transfer.

Acknowledgment. This work is supported by a grant from the National Science Foundation (CHE-8418611). We thank Professor Carl Koval, University of Colorado, for his assistance in the measurements of diffusion coefficients.

Registry No. *trans*-Stilbene, 103-30-0; fumaronitrile, 764-42-1; *trans*-stilbene/fumaronitrile complex, 70152-65-7.

(24) Siders, P.; Cave, R. J.; Marcus, R. A. *J. Chem. Phys.* **1984**, *81*, 5613.
(25) Birks, J. B. *The Exiciplex*; Gordon, M., Ware, W. R., Eds.; Academic: New York, 1975.

pH-Induced Intramolecular Quenching. Ligand-Bridged Complexes Containing Osmium and Ruthenium

Barbara Loeb L.,† Gregory A. Neyhart, Laura A. Worl, Earl Danielson, B. Patrick Sullivan, and Thomas J. Meyer*

Chemistry Department, The University of North Carolina, Chapel Hill, North Carolina 27599, and Faculty of Chemistry, Catholic University, Santiago, Chile *(Received: April 14, 1988)*

In the ligand-bridged complex $[(tpy)(bpy)Os^{II}(4,4'\text{-}bpy)Ru^{II}(H_2O)(bpy)_2]^{4+}$ (tpy is 2,2′:6′,2″-terpyridine; bpy is 2,2′-bipyridine, 4,4′-bpy is 4,4′-bipyridine) and its mixed-valence analogue, pH-induced photophysical effects are observed which are triggered by proton loss from the bound aqua ligand. In the Os(II)–Ru(II)(H_2O) complex, Ru(II) → bpy metal to ligand charge-transfer (MLCT) excitation is followed by rapid, efficient energy transfer to the lower energy Os(III)($tpy^{\bullet-}$) MLCT state. If the pH is raised so that $[(tpy)(bpy)Os^{II}(4,4'\text{-}bpy)Ru^{II}(OH)(bpy)_2]^{3+}$ is the dominant form, the Os(III)$tpy^{\bullet-}$-based emission is quenched by the Ru(II)(OH) site. The mixed-valence complex $[(tpy)(bpy)Os^{III}(4,4'\text{-}bpy)Ru^{II}(H_2O)(bpy)_2]^{5+}$ can be converted from its nonemitting, Os(III)–Ru(II)(H_2O), form, to its emitting form, $[(tpy)(bpy)Os^{II}(4,4'\text{-}bpy)Ru^{III}(OH)(bpy)_2]^{4+}$, by using pH changes to adjust the electronic distribution in the ground state.

Introduction

Recently, it was shown that the electronic distribution within ligand-bridged, mixed-valence complexes can be changed by making changes in the external medium.[1] For example, in the mixed-metal complex, $[(bpy)_2(Cl)Os(pz)Ru(NH_3)_5]^{4+}$ (bpy is 2,2′-bipyridine; pz is pyrazine), different degrees of interaction

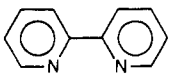
bpy


pz

exist between the Os or Ru sites and the surrounding solvent dipoles. The difference is sufficient that changes in solvent can induce intramolecular electron transfer and a change in the oxidation-state distribution, reaction 1.

$$[(bpy)_2(Cl)Os^{III}(pz)Ru^{II}(NH_3)_5]^{4+} \rightleftharpoons [(bpy)_2(Cl)Os^{II}(pz)Ru^{III}(NH_3)_5]^{4+} \quad (1)$$

In a second experiment the electronic distribution in a ligand-bridged, mixed-valence complex was changed by varying the pH (tpy is 2,2′:6′,2″-terpyridine and 4,4′-bpy is 4,4′-bipyridine)[2]

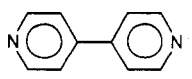
4,4′-bpy

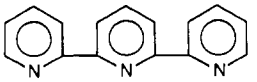
tpy

$$[(tpy)(bpy)Os^{III}(4,4'\text{-}bpy)Ru^{II}(H_2O)(bpy)_2]^{5+} \underset{+H^+}{\overset{+OH^-}{\rightleftharpoons}} [(tpy)(bpy)Os^{II}(4,4'\text{-}bpy)Ru^{III}(OH)(bpy)_2]^{4+} \quad (2)$$
(pH = 1.1) (pH = 8.9)

In the pH-dependent example advantage was taken of the increase in acidity of bound water in Ru(III) and the resulting pH dependence of the Ru(III/II) couple to induce intramolecular electron transfer. The ability to manipulate oxidation-state distribution by changes in pH is possible because there is a change in pK_a between oxidation states. For example, $pK_{a1} = 13.1 \pm 0.1$ for $[Ru(NH_3)_5(H_2O)]^{2+}$ and 4.1 ± 0.1 for $[Ru(NH_3)_5(H_2O)]^{3+}$.[3] The conversion of an aqua to an hydroxo ligand stabilizes the higher oxidation state and lowers the potential of the Ru(III/II) couple. For example, for the couples $[(bpy)_2(py)Ru(H_2O)]^{3+/2+}$ and $[(bpy)_2(py)Ru(OH)]^{2+/+}$, $E^{\circ\prime} = 0.78$ (pH <1) and 0.24 V (pH >11) vs SCE at 22 ± 2 °C, $\mu = 0.1$ M.[4] For the latter case, in the intermediate pH range between $pK_{a1} = 0.8$ for Ru(III) and $pK_{a1} = 10.8$ for Ru(II), the Ru(III/II) couple is pH dependent.

$$[(bpy)_2(py)Ru^{III}(OH)]^{2+} + H^+ + e \rightarrow [(bpy)_2(py)Ru^{II}(OH_2)]^{2+}$$

For the ligand-bridged complex in reaction 2, the Os(III/II) couple is pH independent and the Ru(III/II) couple is pH dependent. This fact allows the site of oxidation, whether at Ru or Os, to be controlled by pH changes. In a closely related experiment it was shown that in the twice oxidized ligand-bridged complex, a chemically reactive $Ru^{IV}{=}O^{2+}$ site can be generated

† Catholic University, Santiago, Chile.

(1) Hupp, J. T.; Neyhart, G. A.; Meyer, T. J. *J. Am. Chem. Soc.* **1986**, *108*, 5349.
(2) (a) Neyhart, G. A.; Meyer, T. J. *Inorg. Chem.* **1986**, *25*, 4807. (b) Neyhart, G. A.; Meyer, T. J., manuscript in preparation.
(3) (a) Kuehn, M.; Taube, H. *J. Am. Chem. Soc.* **1976**, *98*, 689. (b) Ford, P.; Rudd, F. P.; Gaunder, R.; Taube, H. *J. Am. Chem. Soc.* **1968**, *90*, 1187.
(4) (a) Moyer, B. A. Ph.D. Dissertation, University of North Carolina at Chapel Hill, 1979. (b) Moyer, B. A.; Meyer, T. J. *Inorg. Chem.* **1981**, *20*, 436. (c) Binstead, R. A.; Meyer, T. J. *J. Am. Chem. Soc.* **1987**, *109*, 3287.

0022-3654/89/2093-0717$01.50/0